Supporting Information

Porous Molecular Conductor: Electrochemical Fabrication of Through-Space Conduction Pathways among Linear Coordination Polymers

Liyuan Qu,[†] Hiroaki Iguchi,*[,†] Shinya Takaishi,[†] Faiza Habib,[†] Chanel F. Leong,[‡] Deanna M. D'Alessandro,[‡] Takefumi Yoshida,[§] Hitoshi Abe,[∥,⊥] Eiji Nishibori,[#] Masahiro Yamashita*[,†,¶,⊗]

[†]Department of Chemistry, Graduate School of Science, Tohoku University, 6-3 Aza-Aoba, Aramaki, Sendai 980-8578, Japan

[‡]School of Chemistry, The University of Sydney, New South Wales 2006, Australia

[§]Electronic Functional Macromolecules Group, National Institute for Materials Science (NIMS), 1-1 Namiki, Tsukuba, Ibaraki 305-0044, Japan

[∥]Institute of Materials Structure Science High Energy Accelerator Research Organization (KEK), 1-1 Oho, Tsukuba, Ibaraki 305-0801, Japan

[⊥]Department of Materials Structure Science, School of High Energy Accelerator Science, SOKENDAI (the Graduate University for Advanced Studies), 1-1 Oho, Tsukuba, Ibaraki 305-0801, Japan

[#]Division of Physics, Faculty of Pure and Applied Sciences & Tsukuba Research Center for Energy Materials Science (TREMS), University of Tsukuba, Tsukuba, Ibaraki 305-8571, Japan

[¶]Advanced Institute for Materials Research, Tohoku University, 2-1-1 Katahira, Aoba-ku, Sendai 980-8577, Japan

[⊗]School of Materials Science and Engineering Nankai University, Tianjin 300350, China

Table of Contents

Experimental details

General Experimental Information

All chemicals were used without further purification unless otherwise notified. Electrocrystallization was carried out by using direct current (DC) multisources YAZAWA CS-12Z and 0.3 mm ϕ electrodes made from platinum-iridium alloy wires (Pt:Ir = 80:20). Solid-state IR spectra were collected on a JASCO FT/IR 4200 Fourier Transform Infrared Spectrometer. The absorbance of samples which were dispersed in KBr pellets were acquired in this paper unless otherwise noted. An attenuated total reflection (ATR) method was used with a ZnSe prism for the particular purpose (Figure S4). Solid-state UV-Vis-NIR spectra were recorded on a Shimadzu UV-3100 with the same KBr pellets that were used in IR spectroscopy. ^{1}H NMR measurements were performed on a Bruker AV500 at RT. Thermogravimetry (TG) was measured on a SHIMADZU DTG-60/60H at a heating rate of 5 °C/min under a constant nitrogen flow (0.1 L/min). Powder X-ray diffraction (PXRD) patterns were collected on a Bruker D2 PHASER with Cu Kα radiation (λ = 1.5406 Å) at RT. High resolution multi-temperature PXRD profiles were measured at SPring-8 BL02B2 beamline. The sample temperatures were controlled at 100, 300, and 400 K using a nitrogen gas flow device. The wavelength of incident X-ray was 1.08 Å calibrated by CeO_2 standard sample. The ESR spectrum was acquired by using a JEOL JES-FA100.

Syntheses

Synthesis of *N*,*N'*-di(4-pyridyl)-1,4,5,8-naphthalenetetracarboxdiimide (NDI-py)

NDI-py was synthesized according to the previously reported procedure[S1] with a slight modification. 1,4,5,8-Naphthalenetetracarboxylic dianhydride (NDA) (1.70 g, 6.34 mmol) and 4-aminopyridine (1.25 g, 13.3 mmol) were added to a round-bottom flask equipped with 55 mL *N*,*N*-dimethylfolmamide (DMF). The mixture was then refluxed overnight under an ambient atmosphere. The crude product was collected by filtration and recrystallized from DMF. The final product was collected by filtration and washed with MeOH to remove DMF molecules and finally dried in a desiccator. Yield, 80%. Elemental analysis, Calcd for $C_{24}H_{12}N_4O_4$: C, 68.57; H, 2.88; N, 13.33. Found: C, 68.35; H, 2.88; N, 13.32.

Synthesis of $[Cd(NDI\text{-}py)(OH_2)_4](NO_3)_x{\cdot}n$DMA (**PMC-1**)

NDI-py (20 mg, 0.0476 mmol) and $Cd(NO_3)_2{\cdot}4H_2O$ (100 mg, 0.32 mmol) were dissolved into 5 mL *N*,*N*-dimethylacetamide (DMA). A constant current of 30 μA was

applied to the solution. After two days, dark brown rod-like crystals were isolated from the cathode, and subsequently washed by DMA and ethanol followed by drying in N_2 atmosphere. Because lattice solvent molecules (DMA) were gradually desorbed from the crystals, it was difficult to determine the precise number (*n*). Elemental analysis was performed on the heated sample (**PMC-1h**) as described next.

Preparation of [Cd(NDI-py)]$(NO_3)_x \cdot m H_2O$ (**PMC-1h**)

The fresh crystals of **PMC-1** were mounted into a SHIMADZU DTG-60/60H and heated to 210 °C at a heating rate of 5 °C/min under a nitrogen flow. In order to remove all DMA molecules, the sample was maintained at 210 °C until the weight became constant. The heated sample gradually adsorbed water molecules from the atmosphere during the handling. This partially hydrated compound is denoted **PMC-1h** in this manuscript. The absence of DMA molecules was confirmed by the fact that the signal for DMA disappeared in the NMR spectrum of **PMC-1h** dissolved in d_6-DMSO (Figure S3). The number of nitrate ions (*x*) was calculated as 1.3 ± 0.1 from the elemental analysis as described on page S9.

Electrocrystallization conditions for the synthesis of **PMC-1**

We carried out the electrocrystallization under the wide range of applied current (5–70 μA) and found that 30 μA was the best condition to provide high reproducibility and yield. In addition, the electrocrystallization with twice amount of $Cd(NO_3)_2 \cdot 4H_2O$ (200 mg) did not affect the results. The *x* values were evaluated from the elemental analyses of **PMC-1h**, and it can be concluded that **PMC-1** is reproducibly synthesized in same *x* values of 1.3±0.1 under the particular conditions (applied current, 25 and 30 μA; amount of $Cd(NO_3)_2 \cdot 4H_2O$ in 5mL DMA, 100 and 200 mg). We chose applied current of 30 μA and 100 mg of $Cd(NO_3)_2 \cdot 4H_2O$ as the best condition to synthesize **PMC-1**.

Preparation of [Cd(NDI-py)]$(NO_3)_x \cdot m H_2O$ (**PMC-1s**) by soaking method

The fresh crystals of **PMC-1** were soaked into N_2-bubbled toluene and placed for a week. The product then was collected and dried in N_2 atmosphere.

Single-crystal X-ray structure determination

The diffraction data for **PMC-1** were collected on a Rigaku Saturn 724+ CCD diffractometer equipped with graphite monochromated Mo Kα radiation (λ = 0.7107 Å). The crystal structure was solved using direct methods (SHELXT[S2]) and followed by Fourier synthesis. Structure refinement was performed using full matrix least-squares procedures with SHELXL[S3] on F^2 in the Yadokari-XG 2009 software.[S4] The SQUEEZE method was applied to remove the electron density, which was too dispersed to establish a meaningful molecular structure in the pores.[S5] The CCDC number of crystallographic data for **PMC-1** was assigned to CCDC 1897154.

Electrical conductivity measurement

Variable-temperature conductivity data were collected in a liquid He cryostat of a Quantum Design Physical Property Measuring System (PPMS) MODEL 6000 by using the two-probe method in direct current (DC) mode with Keithley sourcemeter model 2611. The cooling/heating rate was 2 K/min. The single crystals were attached onto the sample puck by gold wires (15 μm ϕ) and carbon paste (Dotite XC-12 in diethyl succinate) along the long direction (crystallographic *c* axis). The pressed pellet samples were prepared with a diameter of 3 mm and thickness between 200 and 400 μm.

Solid-state cyclic voltammetry

The solid-state cyclic voltammetry measurements were carried out using a standard three-electrode cell with an ALS/CH Instruments Electrochemical Analyzer Model 620D. The working electrode was a glassy carbon (GC) electrode. Solid **PMC-1** was transferred to the surface of the GC electrode by the mechanical attachment method.[S6] Platinum and silver wires were used for counter and quasi-reference electrodes, respectively. The potential of the quasi-reference electrode was calibrated by using ferrocene (Fc) as an external standard. The cyclic voltammogram of **PMC-1** was acquired in dried acetonitrile under a nitrogen flow at scan rate of 100 mVs^{-1}.

Spectroelectrochemical (SEC) measurement

SEC measurements were conducted using a CARY5000 UV/Vis/NIR spectrophotometer equipped with a Harrick Omni Diff probe attachment spanning a range of 400 nm to 2000 nm. This electrochemical setup involved an indium tin oxide (ITO) coated glass plate as working electrode, a Pt wire as counter electrode and a silver wire as quasi-reference electrode in an oxygen free Teflon cell, as described in

detail previously.[S7] Diffuse reflectance spectra are reported as the Kubelka-Munk transform, where $F(R) = (1-R)^2/2R$ (R is the diffuse reflectance of the sample as compared to $BaSO_4$).

X-ray absorption fine structure (XAFS) measurement

XAFS spectra of Cd K-edge were recorded at room temperature by using the NW10A stations at the Photon Factory Advanced Ring (PF-AR) in High Energy Accelerator Research Organization (KEK), equipped with a Si(311) double-crystal monochromator, a Pt-coated focusing mirror and a Rh-coated double-mirror system for the removal of higher-order harmonics. The higher-order harmonics reduction was not required for our measurements. Cd K-edge energy was calibrated by using Cd metal foil. The powder sample of each complex (**PMC-1**, **PMC-1h**, and **PMC-1s**) was put on a cellulose tape. The fluorescence measurements for Cd K-edge were performed by using a Lytle detector. Extended X-ray absorption fine structure (EXAFS) of each sample was analyzed by using ATHENA software.[S8]

Crystallographic data of PMC-1

Table S1 Crystallographic details for **PMC-1**

Radiation type, wave length	Mo Kα, 0.71073 Å
Empirical formula	$C_{24}H_{20}N_4O_8Cd$
Formula weight	604.84 g/mol
Crystal system	Hexagonal
Space group	$P6_222$
Crystal size	$0.317 \times 0.024 \times 0.020$ mm^3
Crystal color	Dark brown
Crystal shape	Stick
Unit cell dimensions	a = 19.946(11) Å
	c = 9.529(9) Å
Volume	V = 3283.3(5) Å^3
Temperature	100 K
Z	3
Density (calculated)	0.918 Mg/m^3
Absorption coefficient	0.531 mm^{-1}
R_1, $wR_2[I > 2\sigma(I)]$	0.0839, 0.2276
R_1, wR_2[all data]	0.1524, 0.2609
F(000)	912
Goodness of fit on F^2	1.092
Absolute structure parameter	–0.11(3)

Infrared (IR) spectra of NDI-py, PMC-1 and PMC-1h

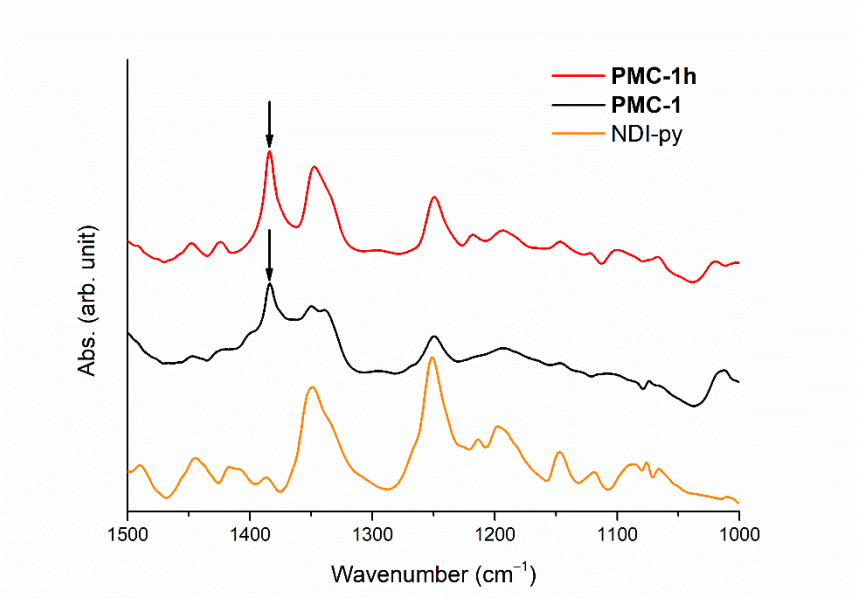

Figure S1 Solid-state IR spectra of NDI-py (orange), **PMC-1** (black) and **PMC-1h** (red). The absorption peaks at 1383 cm^{-1} observed in **PMC-1** and **PMC-1h** correspond to the stretching mode of NO_3^-.

Thermogravimetry (TG) of PMC-1

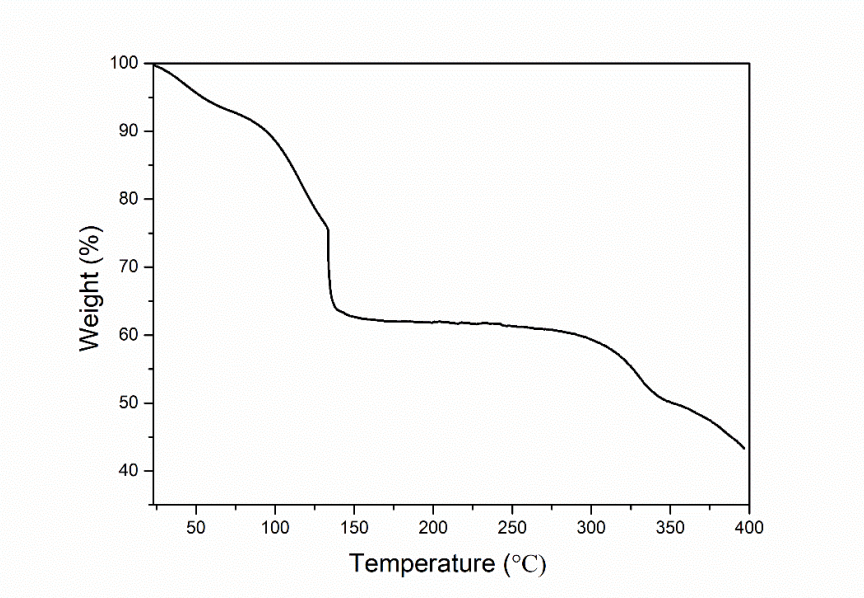

Figure S2 TG analysis of **PMC-1** at a scan rate of 5 K min^{-1}.

NMR spectra of PMC-1 and PMC-1h

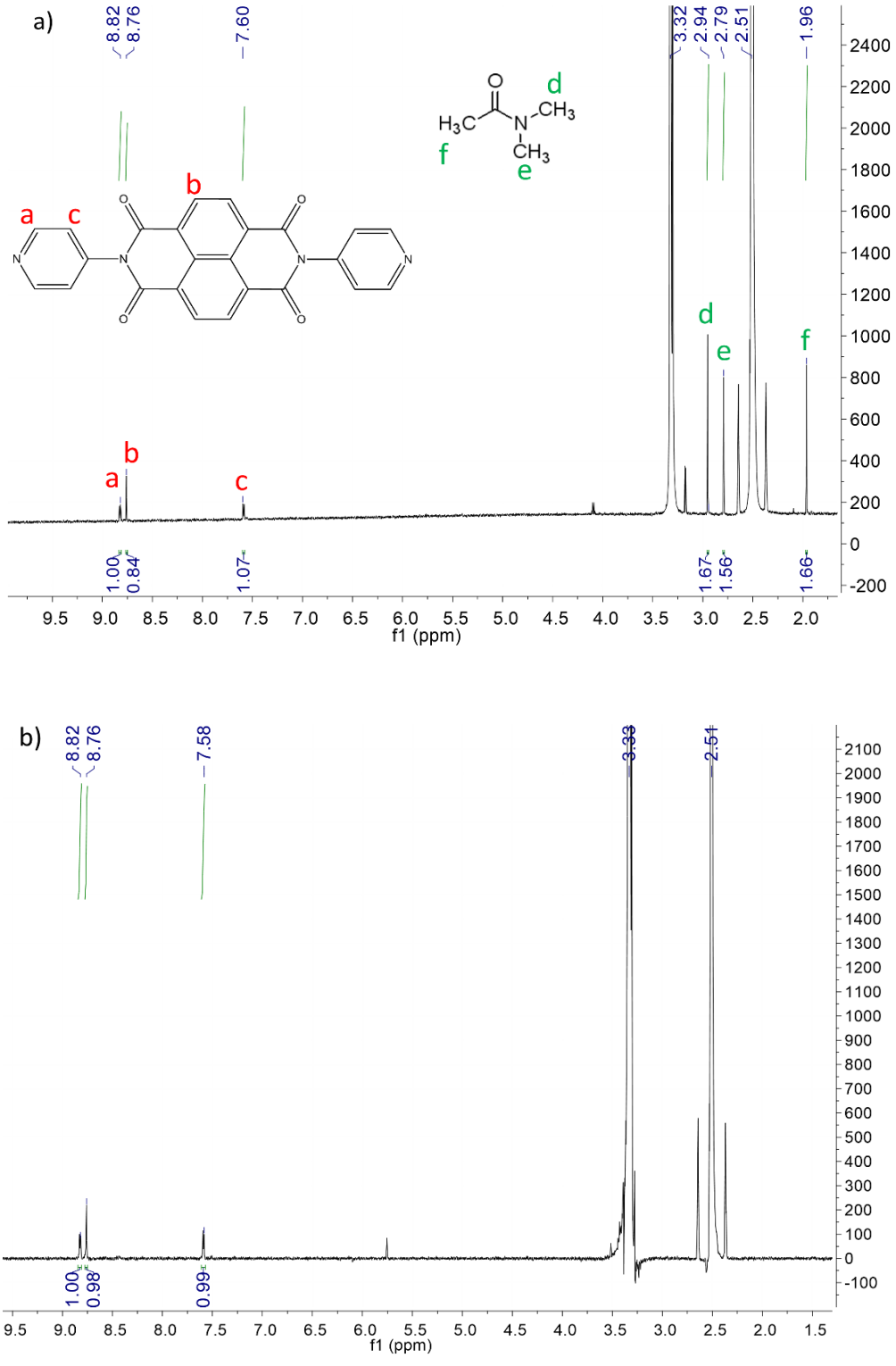

Figure S3 NMR spectra of (a) **PMC-1** and (b) **PMC-1h** dissolved in d_6-DMSO. The peaks at 3.32 and 2.51 ppm correspond to water and residual DMSO molecules in the NMR solvent.

Calculation of the amount of NO_3^- from elemental analyses

Table S2 Elemental analyses of [Cd(NDI-py)]$(NO_3)_x \cdot mH_2O$ (**PMC-1h**) and calculated values with a range of x (= 1.3 ± 0.1) and m values for comparison.

		x	m	C%	H%	N%
Batch 1	**Experimental**			**44.67**	**2.46**	**11.26**
	Calculated	1.2	1.9	44.94	2.48	11.36
		1.3	1.8	44.63	2.43	11.49
		1.4	1.7	44.33	2.39	11.63
Batch 2	**Experimental**			**46.69**	**2.37**	**11.99**
	Calculated	1.2	0.3	47.06	2.07	11.89
		1.3	0.2	46.72	2.03	12.03
		1.4	0.1	46.39	1.98	12.17
Batch 3	**Experimental**			**45.97**	**2.33**	**12.09**
	Calculated	1.2	0.8	46.37	2.21	11.72
		1.3	0.7	46.05	2.16	11.86
		1.4	0.6	45.73	2.11	12.00
Batch 4	**Experimental**			**44.16**	**2.71**	**11.31**
	Calculated	1.2	2.3	44.44	2.58	11.23
		1.3	2.2	44.14	2.53	11.37
		1.4	2.1	43.85	2.48	11.50
Batch 5	**Experimental**			**46.29**	**2.32**	**11.92**
	Calculated	1.2	0.6	46.64	2.15	11.79
		1.3	0.5	46.31	2.11	11.93
		1.4	0.4	45.99	2.06	12.07

PMC-1h does not contain any DMA molecules as shown in Figure S3. Therefore, the excess amount of N atoms can be simply assigned to NO_3^-. The elemental analyses of **PMC-1h** in five different batches show that the calculated values are in good agreement with the experimental ones if the number of NO_3^- (x) is between 1.2 and 1.4. The amount of H_2O molecules (m) was variable because the time for exposure to the atmosphere after the desolvation until the start of elemental analyses was inconsistent. The weak OH stretching mode observed in the IR spectrum with the ATR method (Figure S4) and the weight loss observed in TG (Figure S5) are attributable to the adsorbed H_2O molecules in **PMC-1h**. From the TG analysis, 2% weight loss was found up to 100 °C and can be assigned to 0.7 H_2O molecules (if x = 1.3).

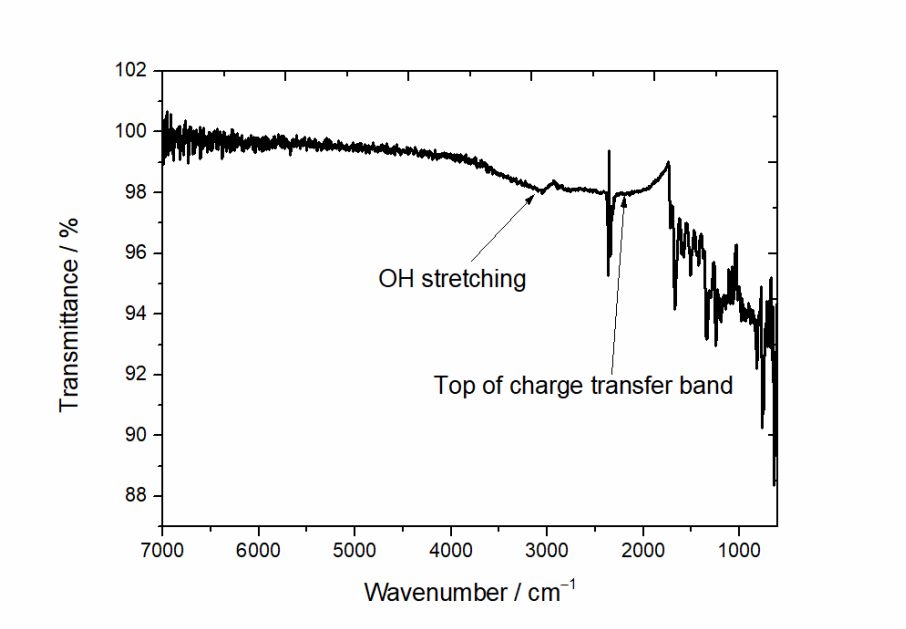

Figure S4 IR spectrum of **PMC-1h** collected in ATR mode.

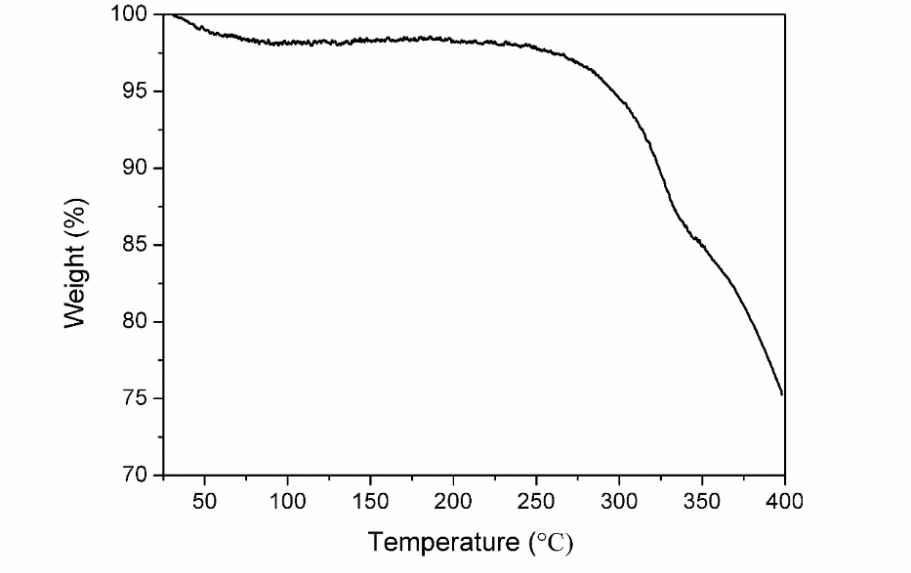

Figure S5 TG trace of **PMC-1h** with a scan rate of 5 °C/min.

ESR spectrum of PMC-1

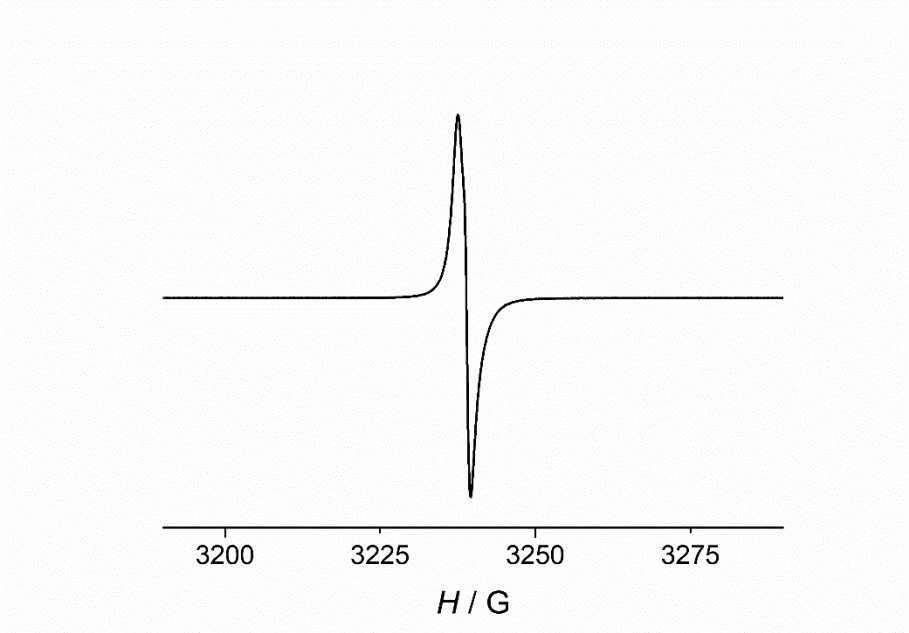

Figure S6 ESR spectrum of **PMC-1** measured at RT.

Solid-state cyclic voltammogram of PMC-1 with *n*-Bu_4NPF_6 electrolyte

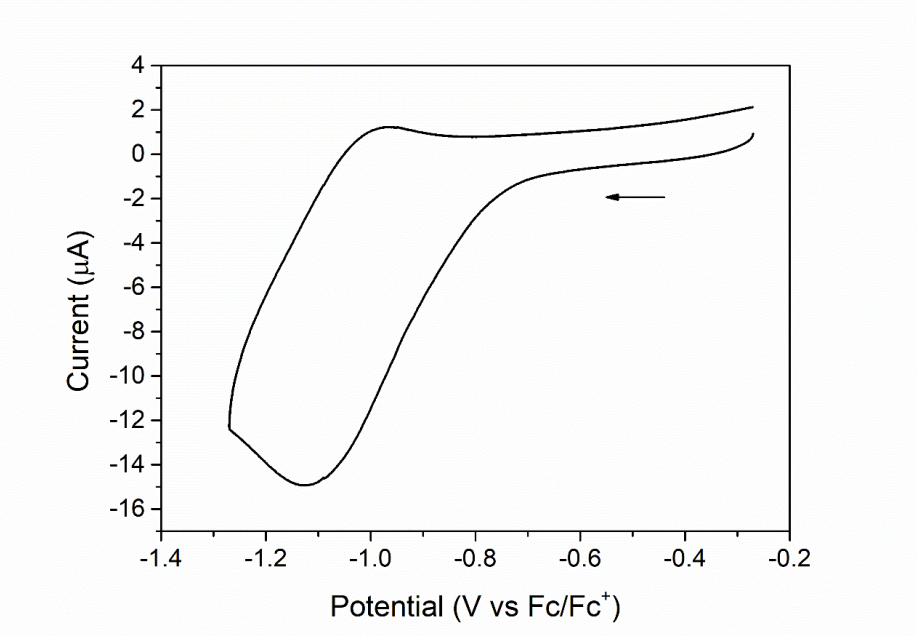

Figure S7 Solid-state Cyclic voltammogram obtained at scan rate of 100 mV/s for reduction of **PMC-1**-modified glassy carbon electrode in contact with 0.1 M *n*-Bu_4NPF_6 in CH_3CN.

Spectroelectrochemistry (SEC) of PMC-1 scanned from –0.9 to 0 V

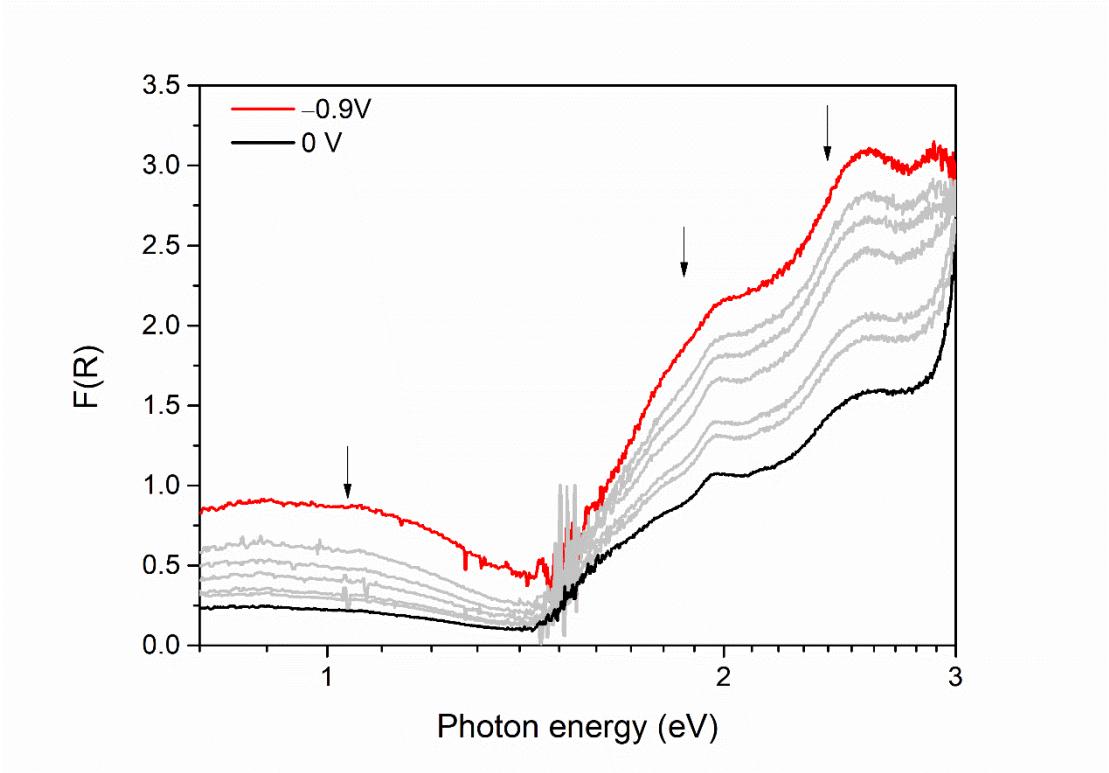

Figure S8 SEC of **PMC-1** in contact with 0.1 M $LiBF_4$ in CH_3CN. The applied potential was scanned from –0.9 V (red) to 0 V (black). Gray lines show the spectral progression and the arrows indicate the direction of this progression.

Electrical conductivity in single crystal and pressed pellet

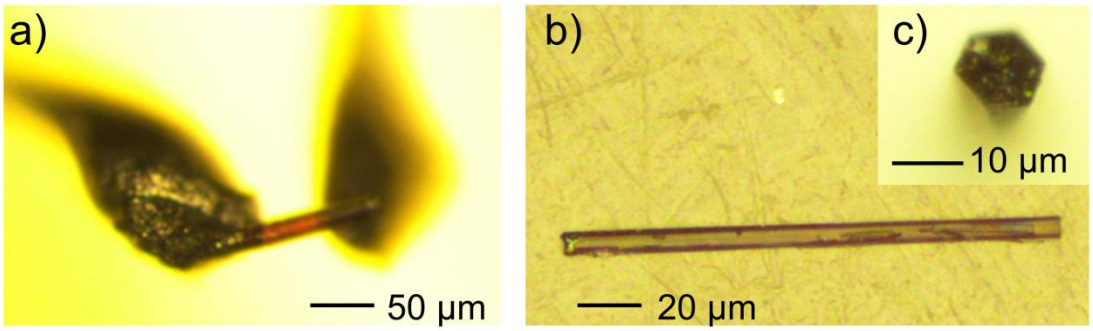

Figure S9 Photographs of **PMC-1** single crystal (a) connected to a gold wire for the measurement of electrical conductivity, (b) a lateral view and (c) hexagonal cross section of **PMC-1**. The crystal morphology indicates that the π-stacked columns grow along the long axis of the single crystal (crystallographic *c* axis).

Table S3 Electrical conductivities of **PMC-1** measured in single crystals.

Batch	1	2	3	4	5
σ_{300K} (S cm^{-1})	1.4×10^{-3}	3.3×10^{-3}	1.1×10^{-3}	2.7×10^{-3}	1.0×10^{-3}

Table S4 Electrical conductivities of **PMC-1** measured in pressed pellets.

Batch	1	2	3
σ_{300K} (S cm^{-1})	1.5×10^{-6}	7.6×10^{-6}	4.2×10^{-6}

Table S5 Electrical conductivities of **PMC-1h** measured in pressed pellets.

Batch	1	2	3	4
σ_{300K} (S cm^{-1})	1.2×10^{-2}	1.7×10^{-2}	3.6×10^{-2}	3.7×10^{-2}

Powder X-ray diffraction (PXRD) patterns of PMC-1 and PMC-1h

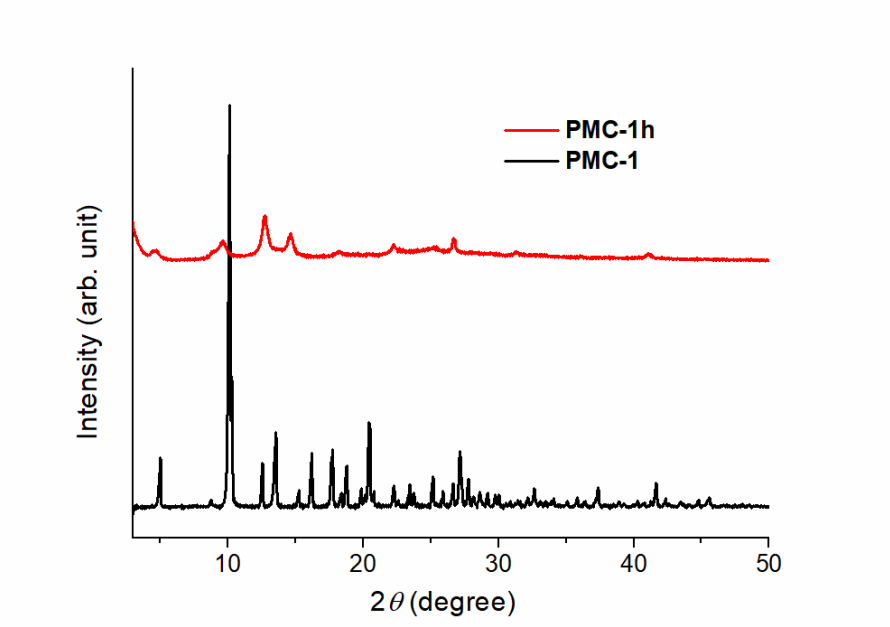

Figure S10 PXRD patterns of **PMC-1** (black) and **PMC-1h** (red).

UV-Vis-NIR spectra of PMC-1 and PMC-1h

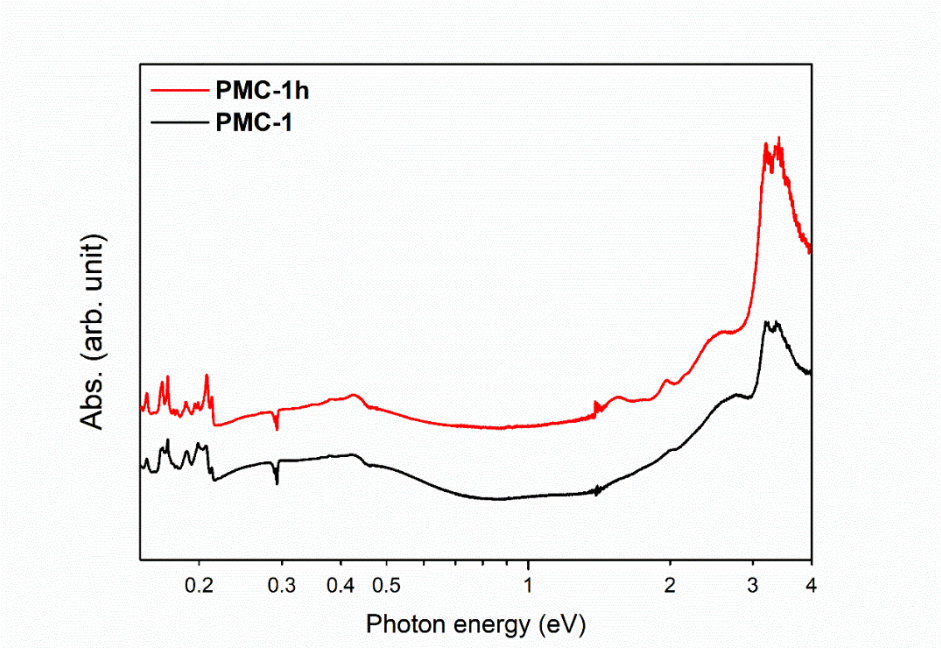

Figure S11 Solid-state UV-Vis-NIR spectra of **PMC-1** (black) and **PMC-1h** (red) dispersed in KBr pellets.

Estimation of the structure of PMC-1h via PMC-1s

It was difficult to discuss the structure of **PMC-1h** directly, because only a few broad peaks were observed in the PXRD pattern as shown in Figure S10. However, the similar but more distinct PXRD pattern (Figure S12) was observed by soaking **PMC-1** in toluene for a week. This sample named "**PMC-1s**" ("s" means "soaked") did not contain DMA as confirmed by the disappearance of the signal of DMA from the ^{1}H NMR spectrum (Figure S13). These results indicate that DMA molecules in the pore of **PMC-1** were extracted to toluene solvent and the structure changed to that isomorphic to **PMC-1h** by soaking process. The crystallinity of **PMC-1s** was higher than that of **PMC-1h** probably because the soaking process was milder than the heating process which was used for the preparation of **PMC-1h**. We also confirmed that the electrical conductivity of **PMC-1s** (pressed pellet) at room temperature was 1.5×10^{-2} S cm^{-1}, which is comparable to that of **PMC-1h**.

In order to discuss the structure of **PMC-1h** via **PMC-1s**, we measured X-ray absorption fine structure (XAFS) spectra (Figure S14) and high resolution PXRD pattern (Figure S16) by using synchrotron X-ray beams. The Fourier transform of extended X-ray absorption fine structure (EXAFS) of **PMC-1**, **PMC-1h**, and **PMC-1s** were almost identical (Figure S15), indicating that all of them have similar six-coordinated octahedral coordination environment around Cd^{2+} ion.

High resolution PXRD patterns of **PMC-1s** were acquired at 100, 300 and 400 K. The peaks are categorized into two groups: (A) sharp peaks which did not shift by temperature change; (B) broad peaks which gradually shifted to small angle as the temperature increased. The crystal lattice and unit cell parameters were estimated to monoclinic P-lattice, a = 7.684 Å, b = 7.733 Å, c = 18.097 Å, β = 92.66°, V = 1074.2 Å^3. The length of the diagonal line of a and c vectors is calculated as 19.986 Å, which is almost identical to the Cd···Cd distance along the linear coordination polymer in **PMC-1** (19.946 Å). Combined with the fact that six-coordinated octahedral coordination geometry in Cd^{2+} is maintained in **PMC-1s**, it is reasonable to consider that $\{\cdots$Cd–(NDI-py)$\cdots\}_\infty$ coordination polymers extend along [-1 0 1] direction. The Miller indexes of all temperature-independent sharp (A) peaks can be assigned as (h 0 l). The temperature-dependent broad (B) peaks are probably assigned to the Miller indexes with $k \neq 0$. Therefore, **PMC-1s** and **PMC-1h** have periodic order of molecules at ac plane but poorly ordered structure along b axis. Although the Rietveld analysis of **PMC-1s** has not yet been successful due to the broad (B) peaks, the large structural change discussed above can induce the enhancement of electrical conductivity in **PMC-1h**. The π-stacked structure was probably changed from 1D columnar to 2D-like packing modes such as brick layer stacking, which can provide higher carrier mobility and lower grain boundary resistivity. Further investigations of the structure of **PMC-1s** by Rietveld analysis and the solvent dependence of structural change are underway.

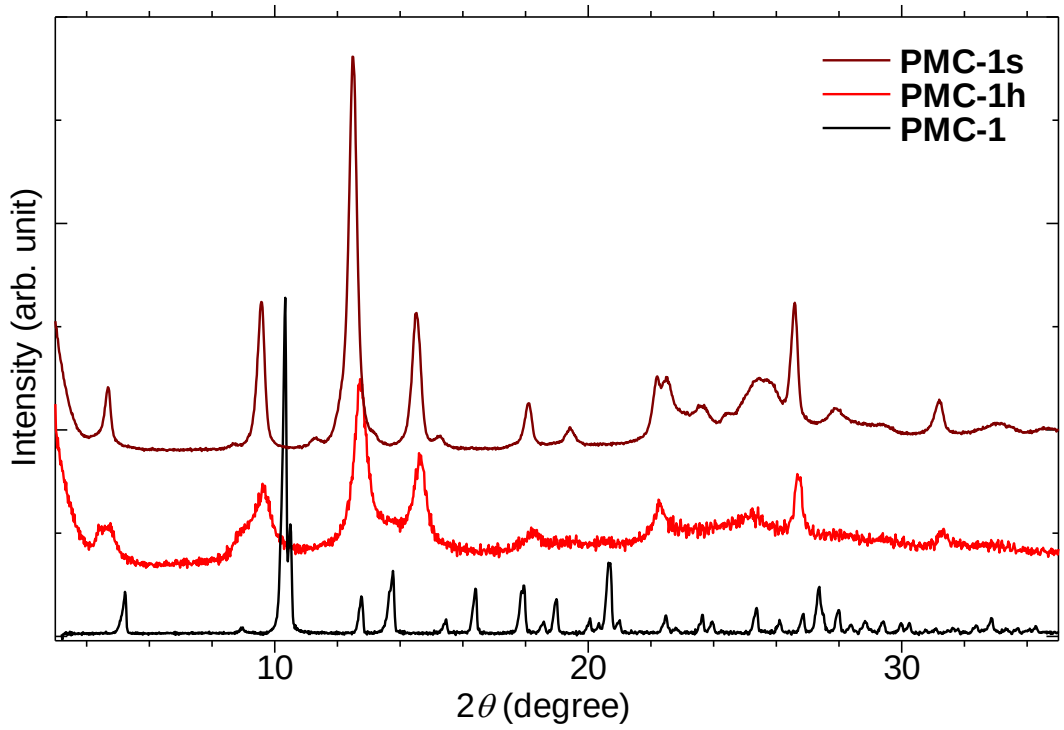

Figure S12 Enlarged PXRD patterns of **PMC-1** (black), **PMC-1h** (red) and **PMC-1s** (brown).

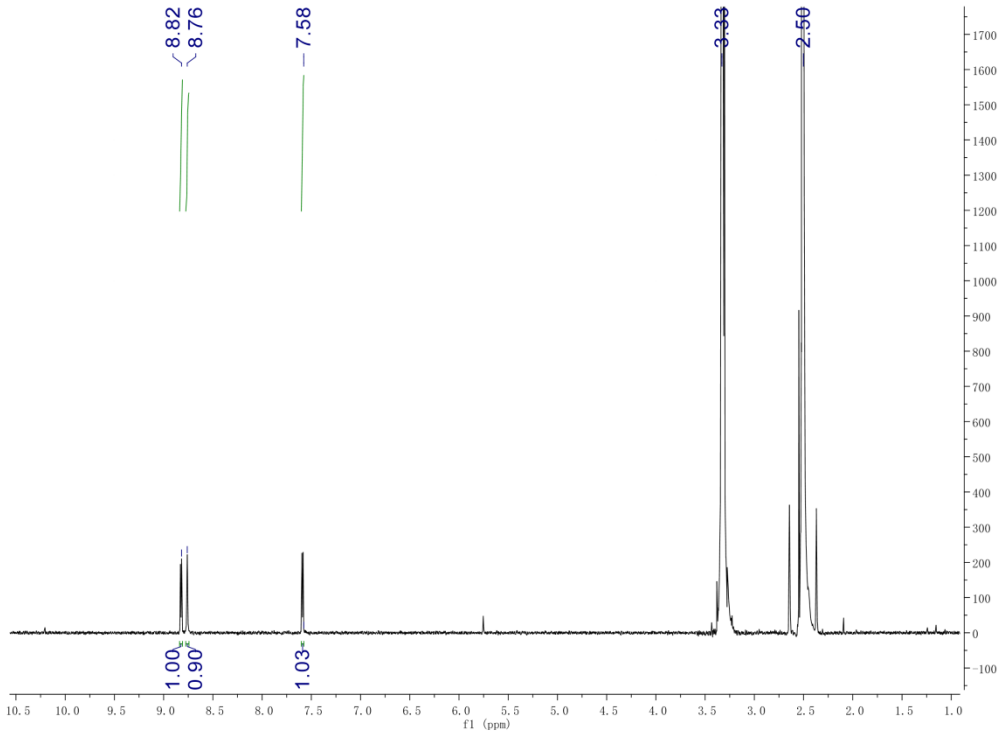

Figure S13 NMR spectrum of **PMC-1s** dissolved in d_6-DMSO. No signal of DMA was observed. Also see Figure S3 for the comparison with **PMC-1** and **PMC-1h**.

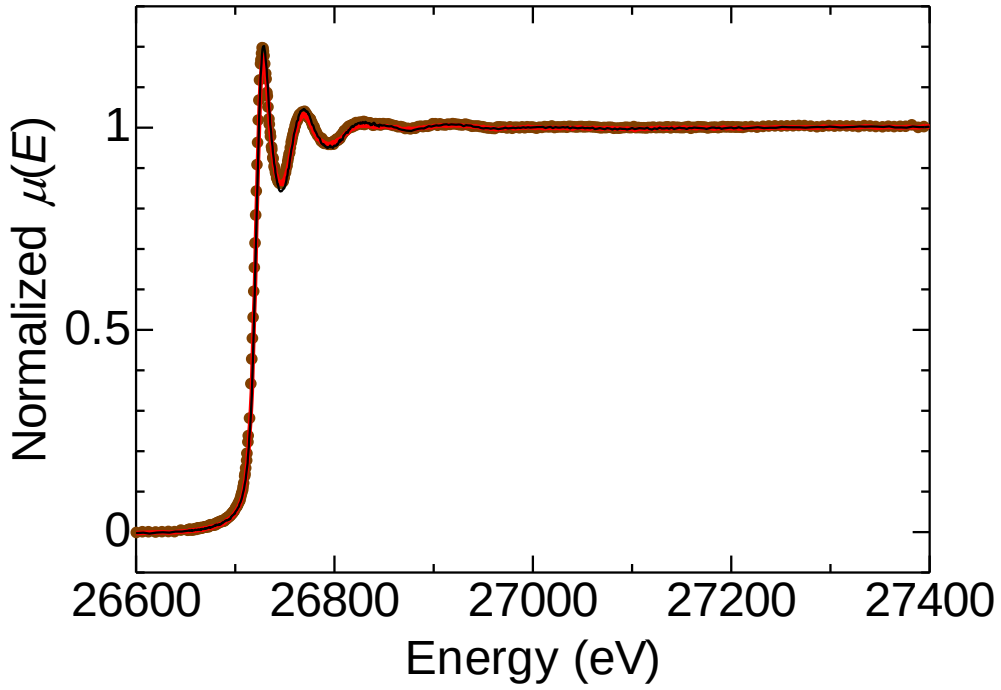

Figure S14 X-ray absorption spectra around Cd-K edge of **PMC-1** (black line), **PMC-1h** (red line) and **PMC-1s** (brown dots).

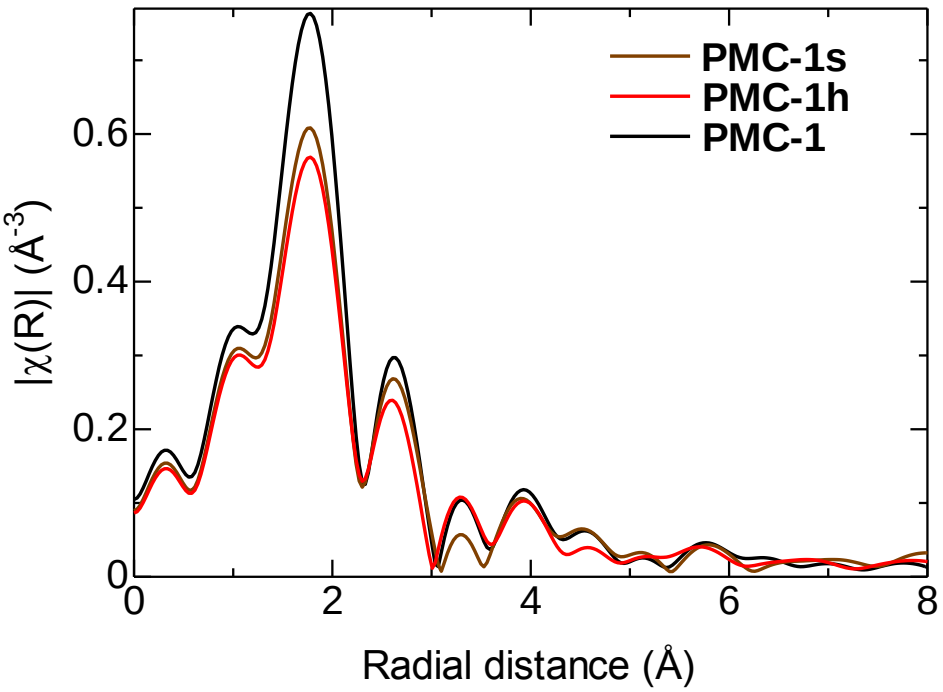

Figure S15 Fourier transformed EXAFS spectra of **PMC-1** (black), **PMC-1h** (red) and **PMC-1s** (brown).

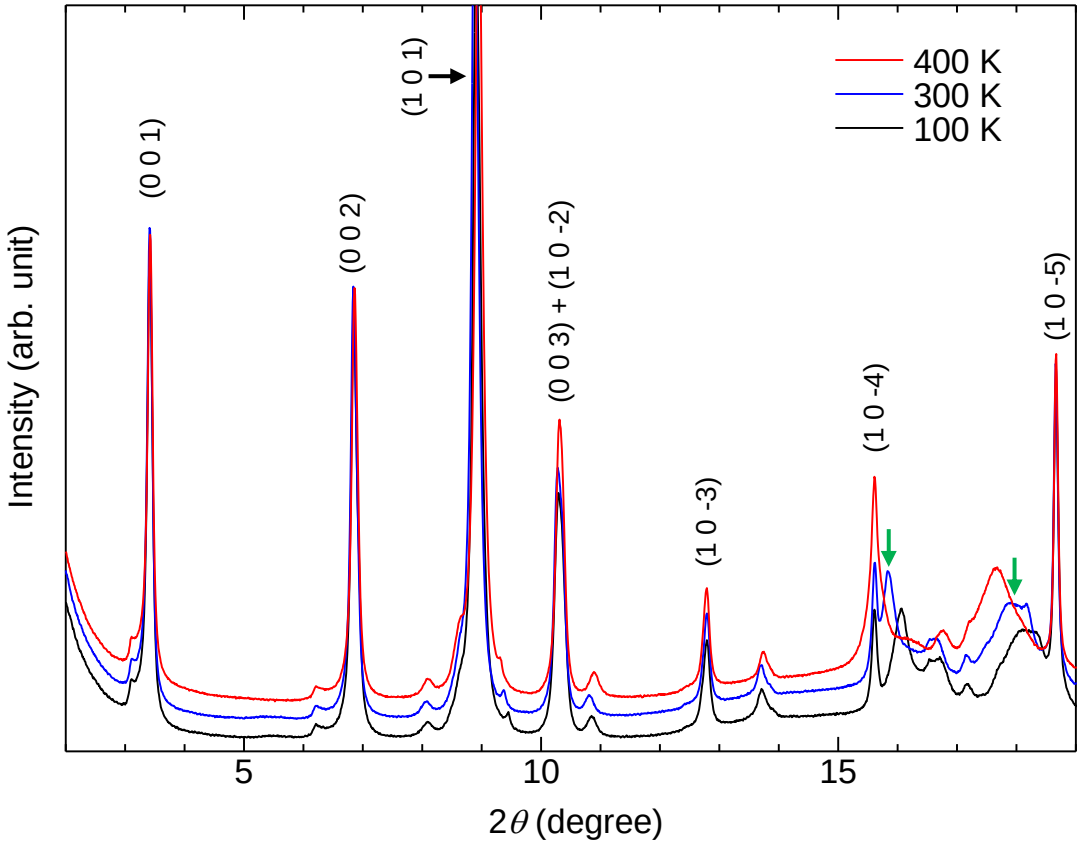

Figure S16 High resolution PXRD patterns of **PMC-1s** measured at 100 K (black), 300 K (blue), and 400 K (red) in SPring-8 BL02B2 beamline (λ = 1.08 Å). The Miller indexes are shown for representative temperature-independent sharp (A) peaks. Green arrows indicate the temperature-dependent broad (B) peaks at 300 K.

References

[S1] Liao, L.-Z.; Wu, X.-Y.; Yong, J.-P.; Zhang, H.-L.; Yang, W.-B.; Yu, R.; Lu, C.-Z. *Cryst. Growth. Des.* **2015**, *15*, 4952–4958.

[S2] Sheldrick, G. M. *Acta Cryst.* **2015**, *A71*, 3–8.

[S3] Sheldrick, G. M. *Acta Cryst.* **2015**, *C71*, 3–8.

[S4] Wakita, K. Yadokari-XG, Software for Crystal Structure Analyses; 2001; Release of Software (Yadokari-XG 2009) for Crystal Structure Analyses, Kabuto, C.; Akine, S.; Nemoto, T.; Kwon, E. *J. Crystallogr. Soc. Jpn.* **2009**, *51*, 218–224.

[S5] Spek, A. L. *Acta Cryst.* **2015**, *C71*, 9–18.

[S6] Iguchi, H.; Nafady, A.; Takaishi, S.; Yamashita, M.; Bond, A. M. *Inorg. Chem.* **2014**, *53*, 4022–4028.

[S7] Usov, P. M.; Fabian, C.; D'Alessandro, D. M. *Chem. Commun.* **2012**, *48*, 3945−3947.

[S8] Ravel B.; Newville, M. *ATHENA, ARTEMIS, HEPHAESTUS: data analysis for X-ray absorption spectroscopy using IFEFFIT*, *J. Synchrotron Radiat.* **2005**, *12*, 537–541.